Department of Aerospace Engineering

AE - 419: Supervised Learning Project

Interplanetary Superhighway

Instructor

Prof. Rohit Gupta,
Department of Aerospace Engineering

Author

Anjali Rawat 190010007

Contents

Nomenclature

$\dot{x}, \dot{y}, \dot{z}$	velocity components of the spacecraft in barycentric coordinate frame
A_Z	out-of plane amplitude of the halo orbit, km
$CR3BP$	circular restricted three body problem
DC	differential correction
IPS	interplanetary superhighway
m	mass of spacecraft
m_1	mass of first primary body: Sun
m_2	mass of second primary body: Earth
r_1	radial distance of third body from 1st primary, normalized units
r_2	radial distance of third body from 2nd primary, normalized units
STM	State Transition Matrix
T	time period of the halo orbit, normalized units
x, y, z	position components of the space craft in barycentric coordinate frame
X	state vector of the spacecraft

1 Abstract

To perform interplanetary travel most missions are designed to make intelligent use of the gravity of various bodies in space to meet mission requirements in a cost effective manner. One such way is to look at the multi body system and make use of the their equilibrium points, known as Lagrange points. Instead of going against gravity, we go along the flow of gravity through paths passing through these Lagrange points. These extremely low cost paths are know as interplanetary superhighways. This report contains the study of the basics of building an interplanetary superhighway like dynamics in a three body system, equilibrium points and a detailed design strategy for the formation of halo orbits near L1 point in the Sun-Earth system.

2 Introduction

A major area of research in orbital mechanics is finding out new, cost effective ways to reach/travel through space within a reasonable time and meeting all requirements of the mission. At the initial stages of my project I read upon various current ongoing research in this field like:

- Space elevators[1] which is a tower or cable, fixed to the Earth at a base station, and rising past geosynchronous orbit, with an anchor at the apex radius, allowing propellant free transfer into space
- Gas Refueling stations[2] at Lagrange Points that will increase a satellite's lifespan and help in reducing space debris
- Interplanetary superhighways to travel into deep space with extremely low fuel

Interplanetary superhighway was selected as the topic for the project. Dynamics in a multi-body system is the base for building such a path and plays a crucial role in all real life missions. The orbits around these liberation points are called halo orbits. The observations from the periodic orbits unravel many mysteries surrounding the universe. The spacecrafts placed around the Sun–Earth L1 point can monitor solar activity and those at L2 point can be used as space observatories for deep space exploration that is why James Webb telescope has been placed in L2 point. The orbits around the Earth–Moon liberation points have been proposed as suitable for communication between Earth and the far side of the moon.

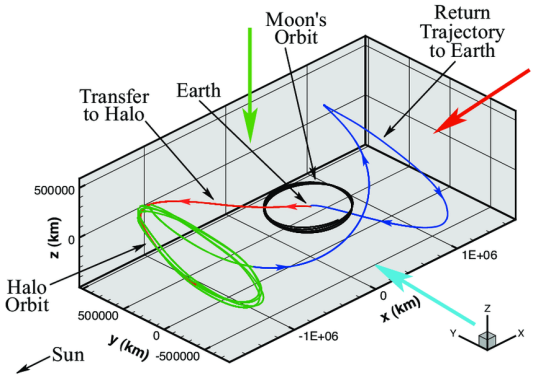

Figure 1: The Genesis Discovery Mission trajectory [8]

Genesis is a solar wind sample return mission as shown in Fig.1 is one of NASA's first robotic sample return missions launched to a halo orbit in the vicinity of the Sun-Earth L1 Lagrange point. The designing of periodic halo orbits at Lagrange points will be looked upon in this report.

3 Literature Review

In order to understand the concept, some papers related to Interplanetary superhighway and design of Halo orbits were read. Rausch in his thesis[3] works upon orbit transfer trajectories from Earth to Halo orbits. [4] examines the formation of halo-orbits by a spacecraft around L1 and L2 libration points of the Sun-Earth system. [5] In this survey methods for designing the periodic orbits around collinear libration points as well as associated invariant manifolds are considered. [6] presents methods for numerical computation of halo orbits and transfer trajectories using differential evolution. Many books related to this concept were also read which are mentioned in the references.

4 Interplanetary Superhighway

4.1 Trajectory of Comet Oterma

From 1910 to 1980, comet Oterma had an encounter with Jupiter which put it on the inside of Jupiter's orbit. Then it had another encounter and it went out of Jupiter's orbit naturally. This was the first instance where a comet jumping from inside to outside of a planet's orbit was discovered. Fig.2 views it in an inetial and comoving frame which is moving along with Jupiter, such that Jupiter and Sun appears to be fixed. Such natural movement of comets in space inspires designing trajectories for spacecrafts so that we can go in and come out of a planets' sphere of influence without any fuel. The interplanetary transport network with gravitational corridors criss-crossing the solar system, influences the fate of comets, asteroids, and Kuiper belt objects.

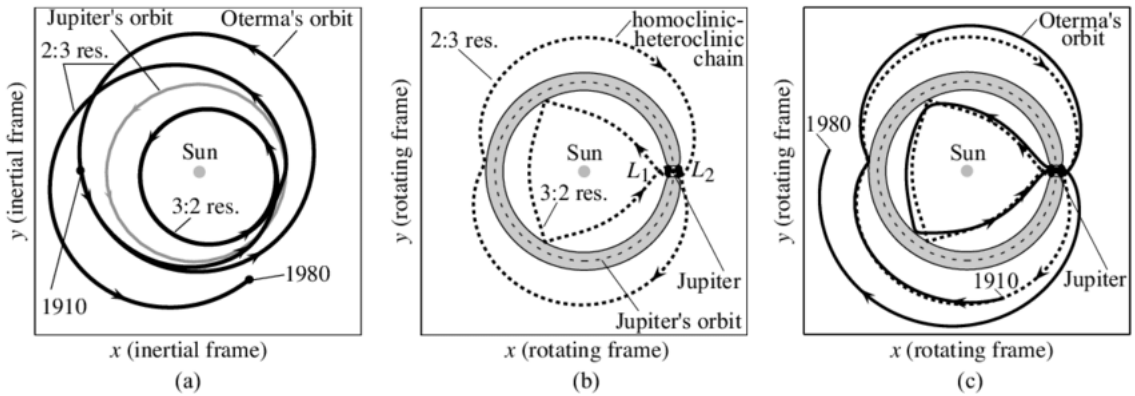

Figure 2: Comet Oterma's trajectory in different frames [14]

4.2 The Interplanetary Transport Network

The Interplanetary Transport Network not only influences the fate of comets, but also facilitate the exploration of the Moon, the asteroids, and the outer solar system. The competing gravitational pull between celestial bodies leads to our Solar System getting interconnected by a vast system of winding tunnels and conduits in space around the Sun and planets which we call the "Interplanetary Superhighway" or IPS for short. This ancient and giant labyrinth around the Sun is generated by the Lagrange Points of all of the planets and satellites within the Solar System. For every Three Body System (such as the Sun-Planet-Spacecraft system), there are five equilibrium points called Lagrange Points (also known as liberation points). They were discovered by Euler (L1, L2, L3) and Lagrange (L4, L5).

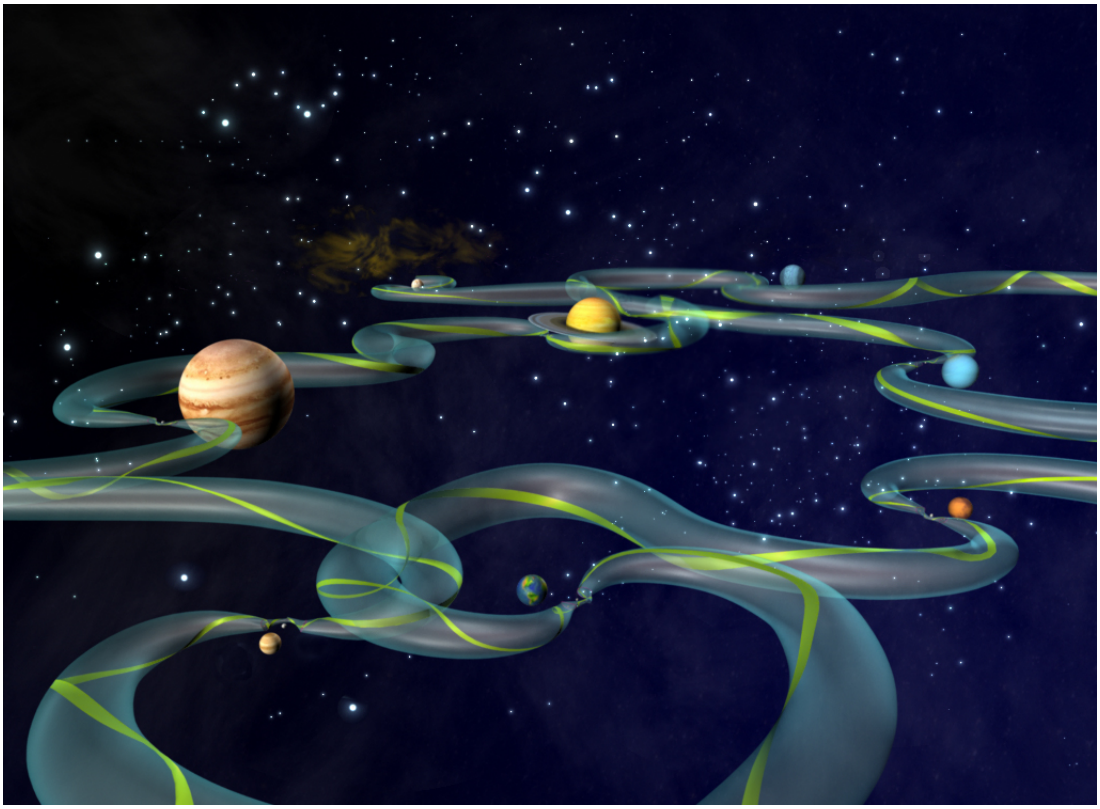

Figure 3: Artist (Cici Koenig) expression of the Interplanetary Transport Network: *It shows the (often convoluted) path through the Solar System. The green ribbon represents one path from among the many that are mathematically possible along the surface of the darker green bounding tube* [15]

The surface of the tunnel in Fig.3 is generated by all the trajectories that asymptotically wind onto the halo orbit without any maneuver. This tube-like surface is called the stable manifold in Dynamical Systems Theory. Similarly, there is a set of trajectories which asymptotically wind off of the halo orbit without any maneuvers. This tunnel is called the unstable manifold as seen in Fig.4.

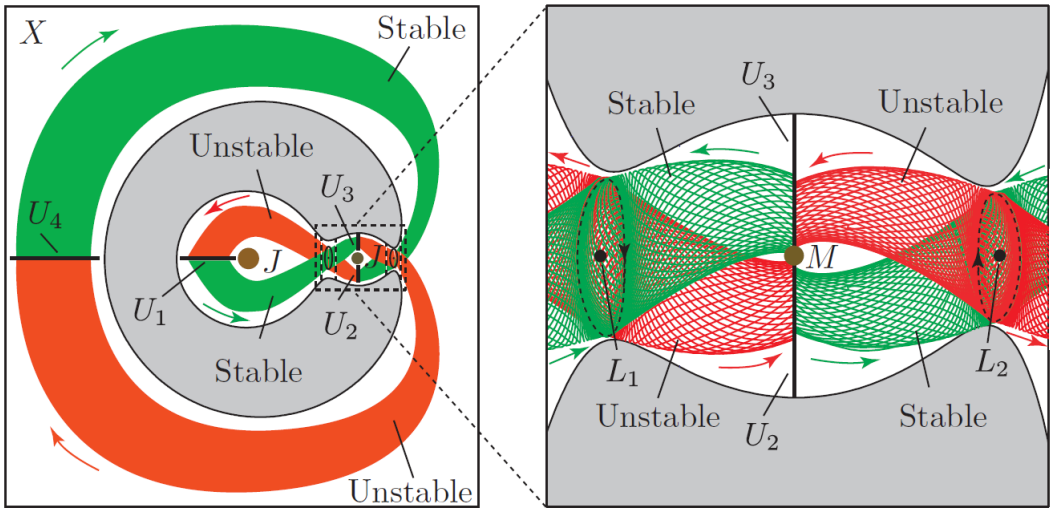

Figure 4: Stable and Unstable Manifolds [8]

5 Circular Restricted Three body Problem

It is important to study the dynamics of a spacecraft in a three body system as it forms the basics for building an IPS. It is not possible to obtain a closed form solution for the general three body problem. However, with some restrictions and computational tools, accurate simulations are possible. In a CR3BP we restrict the motion of the bodies according to the following assumption:

- Both bodies move with a constant angular velocity in circular orbits about their centre of mass
- The third body has negligible mass

Reasonably accurate results can be obtained for low eccentricity systems. In the Earth-Moon system, the Moon has an eccentricity of 0.0549 and in Sun-Earth system, Earth has an eccentricity of 0.01671 and can be considered nearly circular.

The effects of eccentricity are ignored in the circular restricted three-body problem, but perturbations from even small eccentricities can have larger influences than radiation pressure and gravity of the sun. Therefore, except for special cases, the circular restricted three-body problem is generally inaccurate. To account for these eccentric perturbations, dynamic form of distance and angular velocity are used. This type of model is known as the **The Elliptic Restricted Three-Body Problem** The Moon's relatively small eccentricity (0.0549) can drastically perturb satellites over time and complicates calculations significantly.

In Fig. 5 consider two bodies m_1 and m_2 moving under just their mutual gravitation, and let their orbit around each other be a circle of radius r_{12}. View the problem from a non inertial, co-moving frame of reference xyz whose origin lies at the center of mass G of the two-body system, with the x axis directed toward m_2. The y axis lies in the orbital plane, to which the z axis is perpendicular. In this rotating frame of reference, m_1 and m_2 appear to be at rest. We shall henceforth assume that $m_1 > m_2$, so that body 1 might be the Sun and body 2 the Earth.

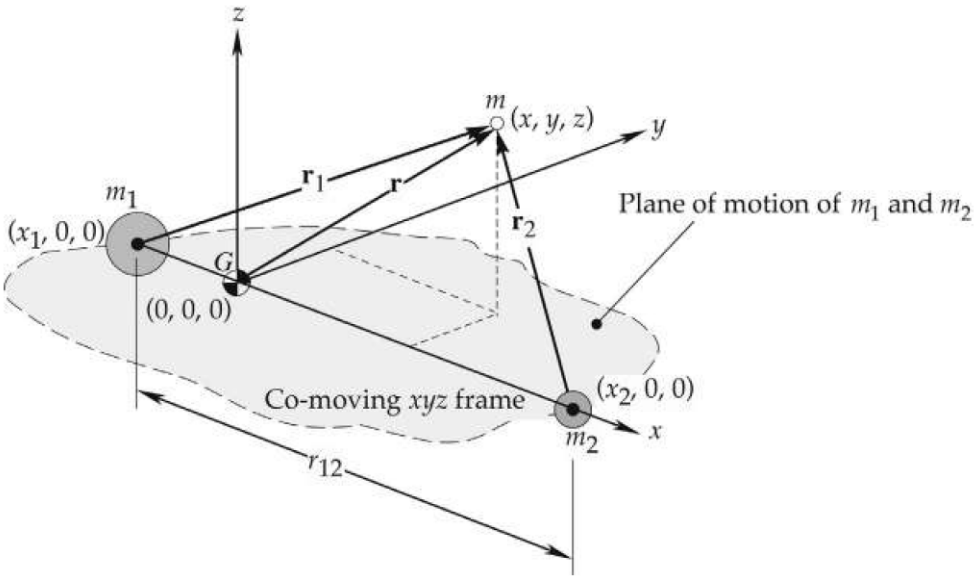

Figure 5: The three body problem viewed in a co-moving frame [10]

The constant, inertial angular velocity ω is given by

$$\boldsymbol{\omega} = \omega \hat{k} \tag{1}$$

where,

$$\omega = \frac{2\pi}{T}$$

where T is the time period of the orbit.

$$T = \frac{2\pi}{\sqrt{\mu}} r_{12}^{3/2}$$

Thus,

$$\omega = \sqrt{\frac{\mu}{r_{12}^3}} \tag{2}$$

The total mass of the system:

$$M = m_1 + m_2 \tag{3}$$

$$\mu = GM \tag{4}$$

The y and z coordinates of m_1 and m_2 are zero and their locations on the x axis can be found using centre of mass equation:

$$m_1 x_1 + m_2 x_2 = 0 \tag{5}$$

The coordinate of Earth (m_2) can be defined as:

$$x_2 = x_1 + r_{12} \tag{6}$$

From Eqs.5,6, we obtain:

$$x_1 = -\pi_2 r_{12} \tag{7}$$

$$x_2 = \pi_1 r_{12} \tag{8}$$

where the dimensionless mass ratios π_1 and π_2 are given by

$$\pi_1 = \frac{m_1}{m_1 + m_2} \tag{9}$$

$$\pi_2 = \frac{m_2}{m_1 + m_2} \tag{10}$$

Now lets introduce a third body of mass m, which has negligible mass as compared with the primary masses m_1 and m_2. The small mass of third body has no effect on the circular motion of the primary bodies around each other. The motion of m due to the gravitational fields of m_1 and m_2 is studied.

In the comoving coordinate system, the position vector of the secondary mass m relative to m_1 is given by:

$$\boldsymbol{r_1} = (x - x_1)\hat{\boldsymbol{i}} + y\hat{\boldsymbol{j}} + z\hat{\boldsymbol{k}} = (x + \pi_2 r_{12})\hat{\boldsymbol{i}} + y\hat{\boldsymbol{j}} + z\hat{\boldsymbol{k}} \tag{11}$$

Relative to m_2 the position of m is:

$$\boldsymbol{r_2} = (x - \pi_1 r_{12})\hat{\boldsymbol{i}} + y\hat{\boldsymbol{j}} + z\hat{\boldsymbol{k}} \tag{12}$$

Relative to the center of mass the position of m is:

$$\boldsymbol{r} = x\hat{\boldsymbol{i}} + y\hat{\boldsymbol{j}} + z\hat{\boldsymbol{k}} \tag{13}$$

The inertial velocity of m is found by taking the time derivative of Eq.13. Since, the xyz coordinate system is rotating with the angular velocity ω, relative to inertial space, therefore, the time derivatives of the unit vectors $\hat{i}$ and $\hat{j}$ are not zero. Accounting for the rotating frame, we obtain:

$$\dot{\boldsymbol{r}} = \boldsymbol{v_G} + \boldsymbol{\omega} \times \boldsymbol{r} + \boldsymbol{v_{rel}} \tag{14}$$

where v_G is the inertial velocity of the center of mass (the origin of the xyz frame), and v_{rel} is the velocity of m as measured in the moving xyz frame. That is:

$$\boldsymbol{v_{rel}} = \dot{x}\hat{\boldsymbol{i}} + \dot{y}\hat{\boldsymbol{j}} + \dot{z}\hat{\boldsymbol{k}} \tag{15}$$

The "five-term" relative acceleration formula is:

$$\boldsymbol{a} = \boldsymbol{a_o} + \dot{\boldsymbol{\omega}} \times \boldsymbol{r_{rel}} + \boldsymbol{\omega} \times (\boldsymbol{\omega} \times \boldsymbol{r_{rel}}) + \boldsymbol{2\omega} \times \boldsymbol{v_{rel}} + \boldsymbol{a_{rel}} \tag{16}$$

The absolute acceleration of m can be found using Eq.16:

$$\ddot{\boldsymbol{r}} = \boldsymbol{a_G} + \dot{\boldsymbol{\omega}} \times \boldsymbol{r} + \boldsymbol{\omega} \times (\boldsymbol{\omega} \times \boldsymbol{r}) + \boldsymbol{2\omega} \times \boldsymbol{v_{rel}} + \boldsymbol{a_{rel}} \tag{17}$$

$a_G = 0$ as the velocity v_G of the center of mass is constant. $\dot{\omega} = 0$ since the angular velocity of the circular orbit is also constant. Therefore, Eq.17 reduces to:

$$\boldsymbol{\ddot{r} = \omega \times (\omega \times r) + 2\omega \times v_{rel} + a_{rel}} \tag{18}$$

where,

$$\boldsymbol{a_{rel} = \ddot{x}\hat{i} + \ddot{y}\hat{j} + \ddot{z}\hat{k}} \tag{19}$$

Substituting values of ω, v_{rel} , r and a_{rel} into Eq.18 we get the expression for inertial acceleration in terms of quantities measured in the rotating frame:

$$\boldsymbol{\ddot{r}} = (\ddot{x} - 2\omega\dot{y} - \omega^2 x)\hat{\boldsymbol{i}} + (\ddot{y} + 2\omega\dot{x} - \omega^2 y)\hat{\boldsymbol{j}} + \ddot{z}\hat{\boldsymbol{k}} \tag{20}$$

Newton's second law for the secondary body is:

$$\boldsymbol{m\ddot{r} = F_1 + F_2} \tag{21}$$

F1 and F2 are the gravitational forces exerted on m by m_1 and m_2, respectively.

$$F_1 = -\frac{\mu_1 m}{r_1^3}\boldsymbol{r_1} \tag{22}$$

$$F_2 = -\frac{\mu_2 m}{r_2^3}\boldsymbol{r_2} \tag{23}$$

where, $\mu_1 = Gm_1$ and $\mu_2 = Gm_2$

Substituting Eq.22 and Eq.23 into Eq. 21 gives:

$$\ddot{r} = -\frac{\mu_1}{r_1^3}\boldsymbol{r_1} - \frac{\mu_2}{r_2^3}\boldsymbol{r_2} \tag{24}$$

Now we equate Eq.20 and Eqs.24 and also substitute values for r_1 and r_2:

$$(\ddot{x}-2\omega\dot{y}-\omega^2 x)\hat{\boldsymbol{i}}+(\ddot{y}+2\omega\dot{x}-\omega^2 y)\hat{\boldsymbol{j}}+\ddot{z}\hat{\boldsymbol{k}} = -\frac{\mu_1}{r_1^3}[(x+\pi_2 r_{12})\hat{\boldsymbol{i}}+y\hat{\boldsymbol{j}}+z\hat{\boldsymbol{k}}]-\frac{\mu_2}{r_2^3}[(x-\pi r_{12})\hat{\boldsymbol{i}}+y\hat{\boldsymbol{j}}+z\hat{\boldsymbol{k}}] \tag{25}$$

Equating the coefficients of $\hat{i}, \hat{j}$, and $\hat{k}$ on each side of this equation yields the three scalar equations of motion for the circular restricted three-body problem:

$$\ddot{x} - 2\omega\dot{y} - \omega^2 x = -\frac{\mu_1}{r_1^3}(x + \pi_2 r_{12}) - \frac{\mu_2}{r_2^3}(x - \pi r_{12}) \tag{26}$$

$$\ddot{y} + 2\omega\dot{x} - \omega^2 y = -\frac{\mu_1}{r_1^3}y - \frac{\mu_2}{r_2^3}y \tag{27}$$

$$\ddot{z} = -\frac{\mu_1}{r_1^3}z - \frac{\mu_2}{r_2^3}z \tag{28}$$

5.1 Nondimensionalized Equations

To eventually generalize the derived equations and to avoid accuracy issue while coding because of large magnitude numbers, it is advantageous to non-dimensionalize and express fundamental quantities in terms of relevant system parameters. The characteristic dimensional quantities identified in the system are length, time, and mass.

For the CR3BP:

- The reference characteristic length is defined as $r^* = |x_1| + x_2$, the sum of the distance between barycentre and Sun and the distance between barycentre and Earth i.e the distance between the two primaries
- The reference characteristic mass is defined as $m^* = m_1 + m_2$
- Hence characteristic time becomes :

$$t^* = [\frac{(r^*)^3}{Gm^*}]^{1/2} \tag{29}$$

- In standard models for the restricted problem such a value of t^* is selected such that the non dimensional gravitational constant $G = 1$

Nondimensional variables are:

$$\boldsymbol{\mu_2} = \frac{Gm_2}{m^*} = \frac{m_2}{m^*} = \boldsymbol{\mu} \tag{30}$$

$$\boldsymbol{\mu_1} = \frac{Gm_1}{m^*} = \frac{m_1}{m^*} = \mathbf{1} - \boldsymbol{\mu} \tag{31}$$

$$\boldsymbol{r_{12}} = r_{12}/r^* = (|x_1| + x_2)/r^* = \mathbf{1} \tag{32}$$

$$\boldsymbol{x_2} = \pi_1 r_{12} = \frac{m_1}{m_1 + m_2} = \mathbf{1} - \boldsymbol{\mu} \tag{33}$$

$$|\boldsymbol{x_1}| = \pi_2 r_{12} = \frac{m_2}{m_1 + m_2} = \boldsymbol{\mu} \tag{34}$$

$$\boldsymbol{M} = M/m^* = (m_1 + m_2)/m^* = \mathbf{1} \tag{35}$$

$$\boldsymbol{\omega} = [\frac{G(m_1 + m_2)}{(r^*)^3}]^{1/2} = \mathbf{1} \tag{36}$$

$$t = t/t^* \tag{37}$$

Putting all these values in Eqs. 24, 25, 26 we get the nondimensionalized CR3BP equations of motion:

$$\ddot{x} = x + 2\dot{y} - \frac{1-\mu}{r_1^3}(x + \mu) - \frac{\mu}{r_2^3}(x - (1 - \mu)) \tag{38}$$

$$\ddot{y} = y - 2\dot{x} - \frac{1-\mu}{r_1^3}y - \frac{\mu}{r_2^3}y \tag{39}$$

$$\ddot{z} = -\frac{1-\mu}{r_1^3}z - \frac{\mu}{r_2^3}z \tag{40}$$

5.2 Lagrangian Approach

We can also find the equations of motion using Lagrangian Approach. Let XYZ be the inertial frame and xyz be the comoving frame. The angluar velocity of the rotating frame $\omega = 1$

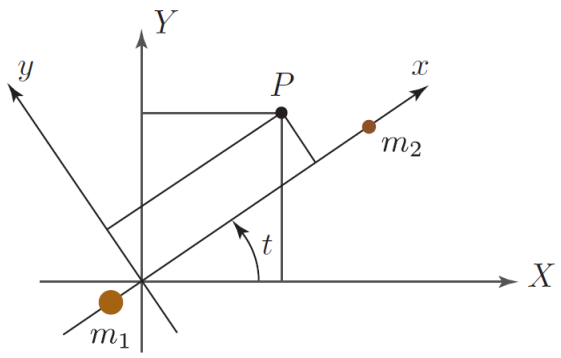

Figure 6: Inertial and Comoving frame [8]

In normalized units, we have the following transformation of the particle's position between the two frames:

$$\begin{pmatrix} X \\ Y \\ Z \end{pmatrix} = A_t \begin{pmatrix} x \\ y \\ z \end{pmatrix}$$

where,

$$A_t = \begin{pmatrix} \cos t & -\sin t & 0 \\ \sin t & \cos t & 0 \\ 0 & 0 & 1 \end{pmatrix}$$

Differentiating gives us the transformation of velocity components from the rotating to the inertial frame:

$$\begin{pmatrix} \dot{X} \\ \dot{Y} \\ \dot{Z} \end{pmatrix} = \dot{A}_t \begin{pmatrix} x \\ y \\ z \end{pmatrix} + A_t \begin{pmatrix} \dot{x} \\ \dot{y} \\ \dot{z} \end{pmatrix}$$

$$= -A_t J \begin{pmatrix} x \\ y \\ z \end{pmatrix} + A_t \begin{pmatrix} \dot{x} \\ \dot{y} \\ \dot{z} \end{pmatrix}$$

$$= A_t \begin{pmatrix} \dot{x} - y \\ \dot{y} + x \\ \dot{z} \end{pmatrix}$$

where, $\dot{A}_t = -A_t J$ and J is:

$$J = \begin{pmatrix} 0 & 1 & 0 \\ -1 & 0 & 0 \\ 0 & 0 & 0 \end{pmatrix}$$

Gravitational Potential
The gravitational potential which the particle experiences due to m_1 and m_2 (in normalized units) is:

$$U = -\frac{\mu_1}{r_1} - \frac{\mu_2}{r_2} - \frac{1}{2}\mu_1\mu_2 \tag{41}$$

The Euler-Lagrange equations are as follows:

$$\frac{d}{dt}\frac{\partial L}{\partial \dot{q}^i} - \frac{\partial L}{\partial q^i} = 0 \tag{42}$$

In rotating frame:

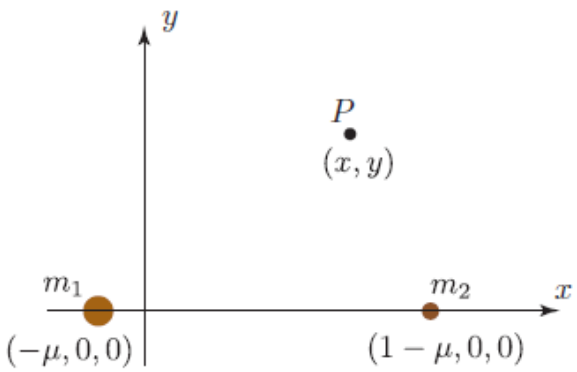

Figure 7: As viewed from comoving frame [8]

$$L(x, y, z, \dot{x}, \dot{y}, \dot{z}) = \frac{1}{2}((\dot{x} - y)^2 + (\dot{y} + x)^2 + \dot{z}^2) - U(x, y, z) \tag{43}$$

where,

$$r_1^2 = (x + \mu_2)^2 + y^2 + z^2 \tag{44}$$

$$r_2^2 = (x - \mu_1)^2 + y^2 + z^2 \tag{45}$$

After solving the above equations we get the same Eqs. 38,39 and 40.

6 Lagrange Points

Lagrange points are the equilibrium points of the three body system. If a spacecraft is kept exactly at one of the Lagrange point then it will appear to be at rest (zero velocity and acceleration) with respect to the other two primaries i.e. in the inertial frame it will appear to be rotating around the Sun along with the Earth with the same angular velocity and maintain the same relative distance from the two.

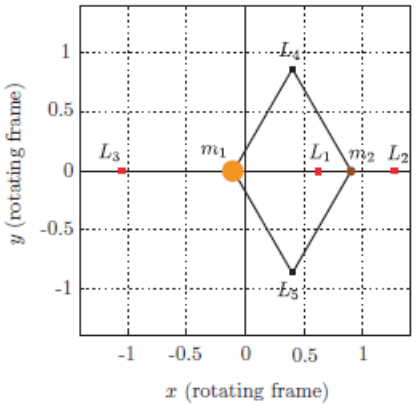

Figure 8: Lagrange points [8]

So for a body at equilibrium points:

$$\dot{x} = \dot{y} = \dot{z} = 0 \tag{46}$$

$$\ddot{x} = \ddot{y} = \ddot{z} = 0 \tag{47}$$

Substituting these into Eqs. 26,27,28:

$$-\omega^2 x = -\frac{\mu_1}{r_1^3}(x + \pi_2 r_{12}) - \frac{\mu_2}{r_2^3}(x - \pi r_{12}) \tag{48}$$

$$-\omega^2 y = -\frac{\mu_1}{r_1^3} y - \frac{\mu_2}{r_2^3} y \tag{49}$$

$$0 = -\frac{\mu_1}{r_1^3} z - \frac{\mu_2}{r_2^3} z \tag{50}$$

From Eq.50 we can conclude that $z = 0$ i.e. equilibrium points lie in the orbital plane.
By solving for x and y using Eqs.48,49 we can find the coordinates of L4/L5:

$$x = \frac{r_{12}}{2} - \pi_2 r_{12} \tag{51}$$

$$y = \pm \frac{\sqrt{3}}{2} r_{12} \tag{52}$$

Therefore, the two primary bodies and these two Lagrange points lie at the vertices of equilateral triangles. The remaining three equilibrium points L1, L2, and L3, are found by setting $y = 0$ as well as $z = 0$. L1,L2 and L3 cannot be found analytically and requires numerical computation using bisection method or Newton Raphson method to find the roots.

6.1 Jacobi Constant

By manipulating the CR3BP equations (Eqs.38,39,40) we get the form:

$$\frac{d}{dt}[\frac{1}{2}v^2 - \frac{1}{2}\omega^2(x^2+y^2) - \frac{\mu_1}{r_1} - \frac{\mu_2}{r_2}] = 0 \tag{53}$$

where, v is the speed of the secondary mass relative to rotating frame:

$$\frac{1}{2}v^2 = \frac{1}{2}\frac{d}{dt}(\dot{x}^2 + \dot{y}^2 + \dot{z}^2) \tag{54}$$

Eq.53 indicates that the bracketed expression is a constant:

$$\frac{1}{2}v^2 - \frac{1}{2}\omega^2(x^2+y^2) - \frac{\mu_1}{r_1} - \frac{\mu_2}{r_2} = C \tag{55}$$

$\frac{v^2}{2}$ is the kinetic energy per unit mass relative to the rotating frame. $-\frac{\mu_1}{r1}$ and $-\frac{\mu_2}{r2}$ are the gravitational potential energies of the two primary masses. $-\frac{\omega^2(x^2+y^2)}{2}$ may be interpreted as the potential energy of the centrifugal force per unit mass induced by the rotation of the reference frame.
The constant C (which is frequently written as -C/2 in the literature) is known as the Jacobi constant, after the German mathematician Carl Gustav Jacobi (1804–1851), who discovered it in 1836. Jacobi's constant may be interpreted as the **total energy of the secondary particle relative to the rotating frame**. C is a constant of the motion of the secondary mass just like energy and angular momentum are constants of the relative motion in the two-body problem.

Importance of Jacobi Constant
The accuracy of a numerical simulation can be verified by checking that the constant C remains invariant during a simulation.
Another popular use of the Jacobi integral is to establish regions around m_1 and m_2 within which m may travel given its initial states. For unpowered flight, the initial position and velocity vectors determine the resulting trajectory. Through the Jacobi integral, the initial states also determine the value of the constant C. Extreme points on a trajectory are encountered whenever the velocity magnitude v goes to zero. Therefore, setting $v = 0$ in the Jacobi integral for a given energy constant C provides an algebraic expression of all such feasible (x,y,z) "apogee-like" locations:

Solving for v^2

$$v^2 = \omega^2(x^2+y^2) + 2\frac{\mu_1}{r_1} + 2\frac{\mu_2}{r_2} + 2C \tag{56}$$

We know that v^2 is always positive, hence:

$$\omega^2(x^2+y^2) + 2\frac{\mu_1}{r_1} + 2\frac{\mu_2}{r_2} + 2C \geq 0 \tag{57}$$

Trajectories of the secondary body in regions where this inequality is violated are not allowed. The boundaries between forbidden and allowed regions of motion are found by setting $v^2 = 0$. That is:

$$\omega^2(x^2+y^2) + 2\frac{\mu_1}{r_1} + 2\frac{\mu_2}{r_2} + 2C = 0 \tag{58}$$

For a given value of the Jacobi constant the curves of zero velocity are determined by this equation. These boundaries cannot be crossed by a secondary mass (spacecraft) moving within an allowed region.

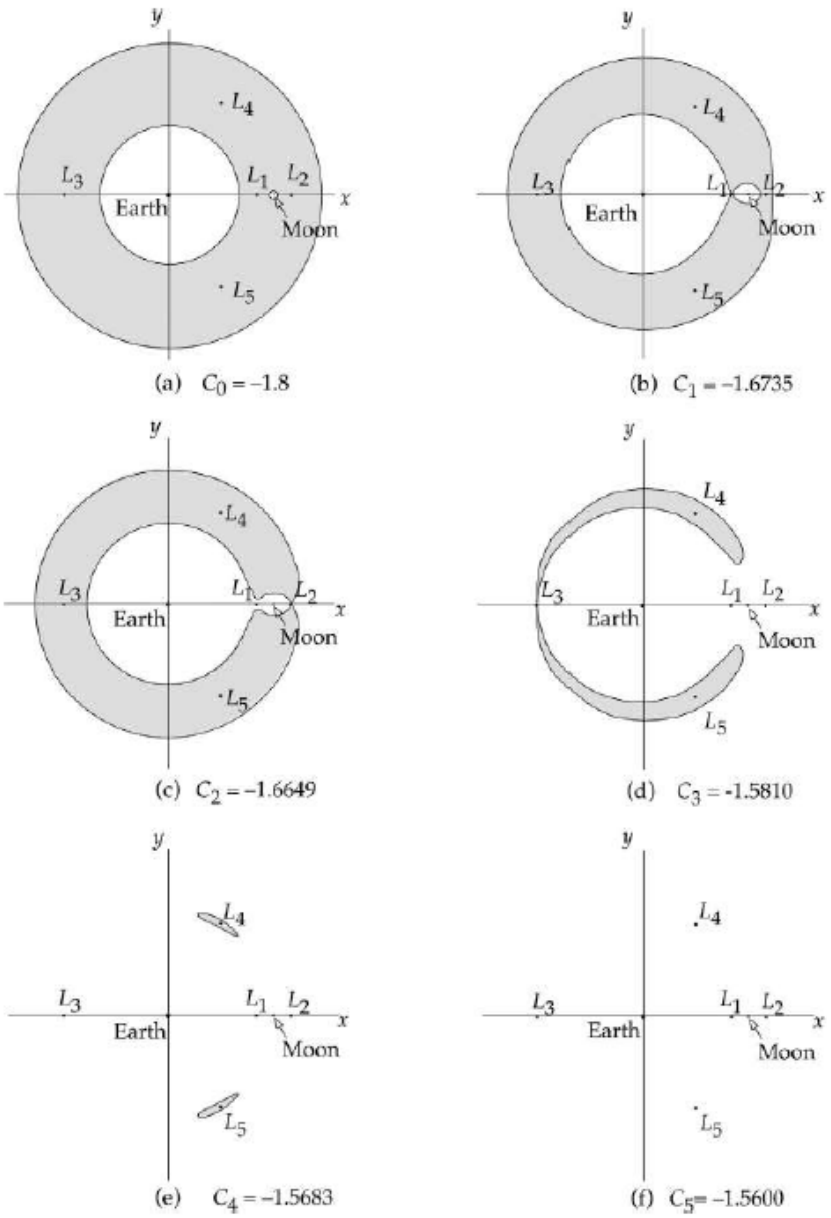

Figure 9: Forbidden regions (shaded) within Earth-Moon system for increasing values of Jacobi's constant [10]

Fig.9 depicts the zero velocity curves for an Earth-Moon system. As C increases the corridor of allowed regions open. Looking at these points from an energy perspective it is evident that L1 represents the least energy state to reach, while the L4 and L5 points require the most energy.

6.2 Stability

Now we focus on the space near the liberation point. If a body starts out at rest near a Lagrange point, will it remain at the vicinity or will it winf off into spcae over time? To answer this question we will study the stability of these L points. Indirect method of Lyapanov is used to study stability of L points i.e. the system is linearized about L points to determine the local stability.

Indirect Method of Lyapanov
Let the system be:

$$\dot{x} = f(x,t) \tag{59}$$

with $f(0,t) = 0$ for all $t \geq 0$.

We define Jacobian matrix of f(x,t):

$$A(t) = \frac{\partial f(x,t)}{\partial x}|_{x=0} \tag{60}$$

The linearized equations of the system (Eq.59) about the origin is:

$$\dot{z} = A(t)z \tag{61}$$

If the system (Eq.59) is time-invariant, then the indirect method says that if the eigenvalues of Jacobian matrix A (Eq.60) are in the open left half complex plane, then the origin is asymptotically stable. Using this concept we linearise the CR3BP equations about liberation points and study the nature of the eigenvalues of their Jacobian Matrices and observe the following:

For colinear points L1,L2,L3:

- For pure motion along the z axis out of the plane, the eigenvalues are purely imaginary. Therefore, the out of plane departure motion is always at least marginally stable.
- For pure x-axis departures, one of the eigenvalues is guaranteed to be positive. Therefore, such radial departure motion is unstable
- For pure y axis departure the eigenvalues are purely imaginary. Therefore tangential y departures are at least marginally stable.

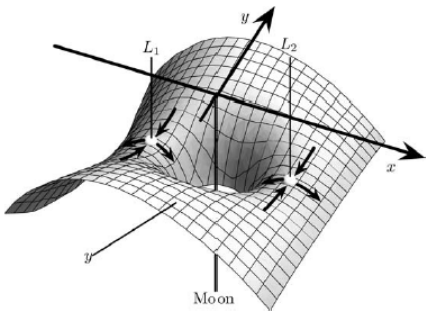

Figure 10: Partial instability of L1 and L2 [9]

Fig.10 visually illustrates why the radial motion about collinear points is unstable. If a spacecraft is attempting to stay at a collinear libration point, the control system would only have to stabilize the radial departure motions.

Motion after deviating considerably from L1 point

The figures below show the 3D and top view of the motion of a body that deviated considerably from L1 point. It enters into a chaotic trajectory and becomes heliocentric after sometime.

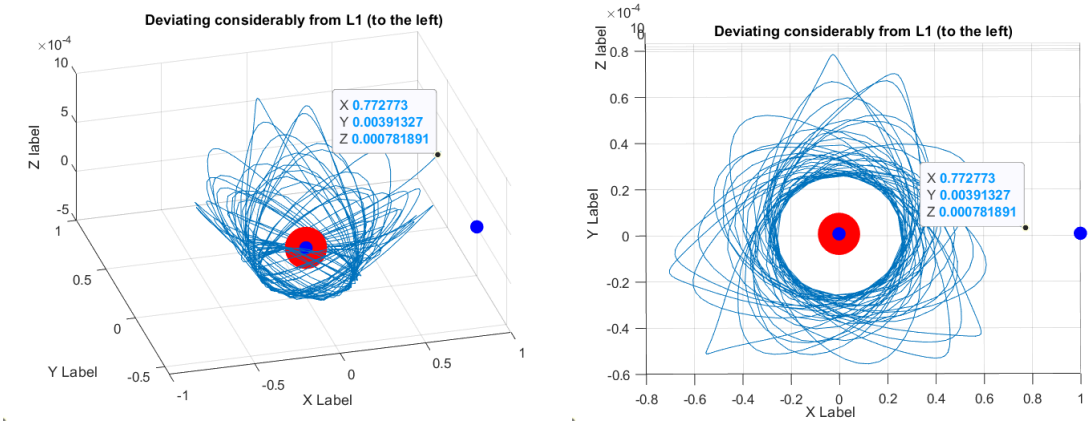

For L4 and L5 points:

- The motion near the L4 and L5 Lagrange libration points is neutrally stable
- They will remaiin stable only when the following condition is met:

$$\frac{m_1}{m_2} + \frac{m_2}{m_1} \geq 25 \tag{62}$$

  That is the larger mass m_1 must be atleast 25 times larger than m_2

- In the sun–Jupiter system a group of asteroids called the Trojans were found in 1906 at the corresponding L4 and L5 libration points. All of these asteroids oscillate in an apparently neutrally stable manner in the vicinity of these stationary points.

Motion at L4/L5 points

The following figures show the motion of spacecraft at L4 point, and demonstrates it neutral stability.

1. The figure on the left shows motion of body for initial conditions exactly at L4 coordinates. Blue unfilled circle marks the position of the body. It remains at L4 and does not spin into space even for longer propagation. Figure on right shows velocity variation for small time. Body seems to oscillate in vicinity of L4.

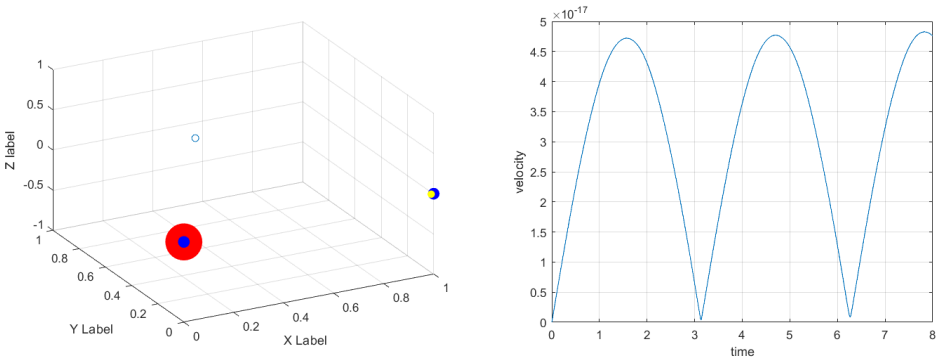

2. The figure on the left shows close up at L4, propagating for t=100. Oscillations are visible but it does not escape L4 vicinity. Figure on right shows velocity variation for t=100 and the velocity seems to increase.

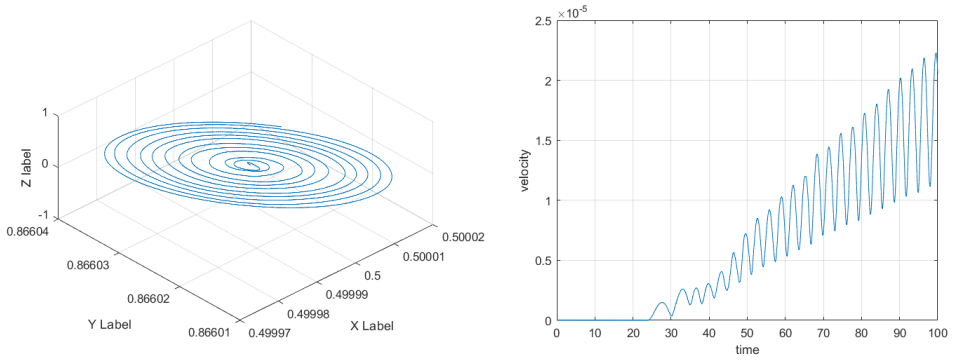

3. The figure on the left shows close up at L4, propagating for t=1000. Oscillations are visible but it does not escape L4 vicinity. Figure on right shows velocity variation for t=1000 and the velocity seems to increase.

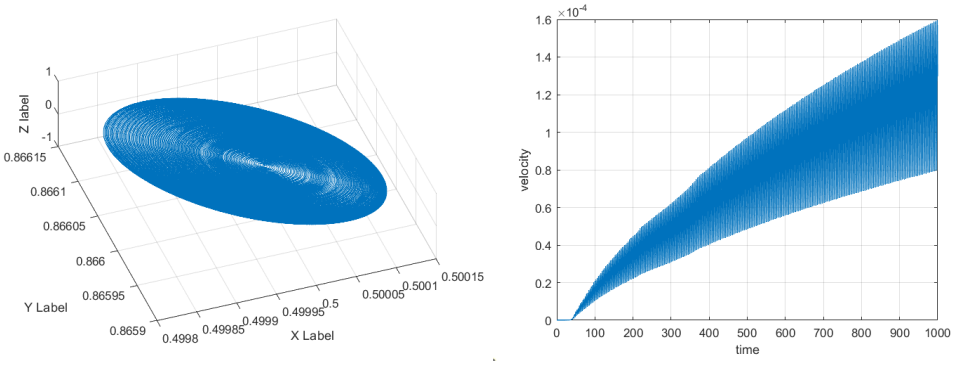

7 Halo orbits

A number of stationary periodic orbits can be found around these liberation points. The main ones being planar and vertical families of Lyapunov periodic orbits; three-dimensional quasi-periodic Lissajous orbits; periodic halo orbits; and quasi-halo orbits. We will be focussing on formation of periodic halo orbit, specifically on the ISEE-3 halo orbit[7].
The mission design to halo orbits involves two major steps:

- The design of halo orbit
- The design of an optimal transfer trajectory to the halo orbit from an parking orbit satisfying certain objectives.

The halo orbit design is conventionally carried out using analytical solutions initially and then refined using a differential correction (DC) scheme.

7.1 Analytical method

Linearized Equations about Sun-Earth system L1 point

After shifting the origin to L1 point and linearising the CR3BP equations about it we get:

$$\ddot{x} - 2\dot{y} - (1 + 2c_2)x = 0 \tag{63}$$

$$\ddot{y} + 2\dot{x} + (c_2 - 1)y = 0 \tag{64}$$

$$\ddot{z} + c_2 z = 0 \tag{65}$$

where, according to Richardson[7]

$$c_2 = \frac{1}{\gamma_L^3}[\mu + \frac{(1-\mu)\gamma_L^3}{(1-\gamma_L^3)}] \tag{66}$$

$$\gamma_L = \frac{r_E}{r^*} \tag{67}$$

where, r_E is the distance between L1 and Earth and r^* is the distance between Sun and Earth. Therefore γ_L is the normalized distance between L1 and Earth.

Looking at the above equations we can comment that the motion in the x-y plane is coupled, while the z axis solution is simple harmonic, since $c_2 > 0$

To compute the eigen values we find the Jacobian matrix of the system:

$$\boldsymbol{X' = AX}$$

Eqs. 63,64 and 65 can be written in the above form as:

$$\begin{pmatrix} \dot{x} \\ \dot{y} \\ \dot{z} \\ \ddot{x} \\ \ddot{y} \\ \ddot{z} \end{pmatrix} = \begin{pmatrix} 0 & 0 & 0 & 1 & 0 & 0 \\ 0 & 0 & 0 & 0 & 1 & 0 \\ 0 & 0 & 0 & 0 & 0 & 1 \\ -(1+2c_2) & 0 & 0 & 0 & -2 & 0 \\ 0 & (c_2-1) & 0 & 2 & 0 & 0 \\ 0 & 0 & c_2 & 0 & 0 & 0 \end{pmatrix} \begin{pmatrix} x \\ y \\ z \\ \dot{x} \\ \dot{y} \\ \dot{z} \end{pmatrix} \tag{68}$$

The eigenvalues come out to be:

$$\lambda^2 = \frac{c_2 - 2 + \sqrt{9c_2^2 - 8c_2}}{2} \tag{69}$$

$$\omega_p^2 = \frac{2 - c_2 + \sqrt{9c_2^2 - 8c_2}}{2} \tag{70}$$

$$\omega_v^2 = -c_2 \tag{71}$$

Hence, the linear behavior near the collinear libration point is of the type ($saddle \times center \times center$) with eigenvalues ($\pm\lambda, \pm i\omega_p, \pm i\omega_v$)

Since the two real roots are opposite in sign, arbitrarily chosen initial conditions will give rise, in general, to unbounded solutions as time increases. If, however, the initial conditions are restricted so that only the non-divergent mode is allowed, the xy-solution will be bounded. In this case, the linearized equations have solutions of the form:

$$x = -A_x \cos(\omega_p t + \phi) \tag{72}$$

$$y = kA_x \sin(\omega_p t + \phi) \tag{73}$$

$$z = A_z \sin(\omega_v t + \psi) \tag{74}$$

where,

$$k = \frac{\omega_p^2 + 1 + 2c_2}{2\omega_p} \tag{75}$$

The linearized motion will become quasi-periodic and produce Lissajous-type trajectories if the in-plane (ω_p) and out of plane (ω_v) frequencies are such that their ratio is irrational, as shown in Fig.11

Amplitude Constraint Relationship:

For halo orbits, the amplitudes A_x and A_z are constrained by a certain non-linear algebraic relationship:

$$l_1 A_x^2 + l_2 A_z^2 + \triangle = 0 \tag{76}$$

l_1, l_2 and $\triangle$ are constants specific to the system (Values given in [7] and [8]). Hence, any halo orbit can be characterized completely by specifying a particular out-of-ecliptic plane amplitude Az.

Phase Angle Relationship:

For halo orbits, the phases ϕ and ψ are related to each other in a linear fashion:

$$\psi - \phi = \frac{m\pi}{2} \tag{77}$$

where, m = 1,3.

For m = 1, Az is positive, and we have the northern (class I) halo whose maximum out-of-plane component is above the xy-plane ($z > 0$), Fig.12. For m = 3, Az is negative, and we have the southern (class II) halo whose maximum out-of plane component is below the xy-plane ($z < 0$),

Fig.13. Northern and southern halo orbits with the same Az amplitude are mirror images across the xy-plane, as seen in Fig.12 and Fig.13.

Halo Orbit Period Amplitude Relationship:

The halo orbit time period can be computed as:

$$T = \frac{2\pi}{n_E \omega_p \omega_v} \tag{78}$$

where, n_E is the mean orbital motion. For Sun-Earth system $n_E = 1.990986606 \times 10^{-7} rad/s$ according to Richardson[7].

7.1.1 Results

The constants used are specific to the system. For the Sun-Earth system the constants (Values given in [7] and [8]) used are :

- $\omega_p = 2.086453455$
- $\omega_v = 2.0152105515$
- $k = 3.2292680962$
- $l_1 = -15.9650314$
- $l_2 = 1.740900800$
- $\triangle = 0.29221444425$

1. When $\omega_p \neq \omega_v$

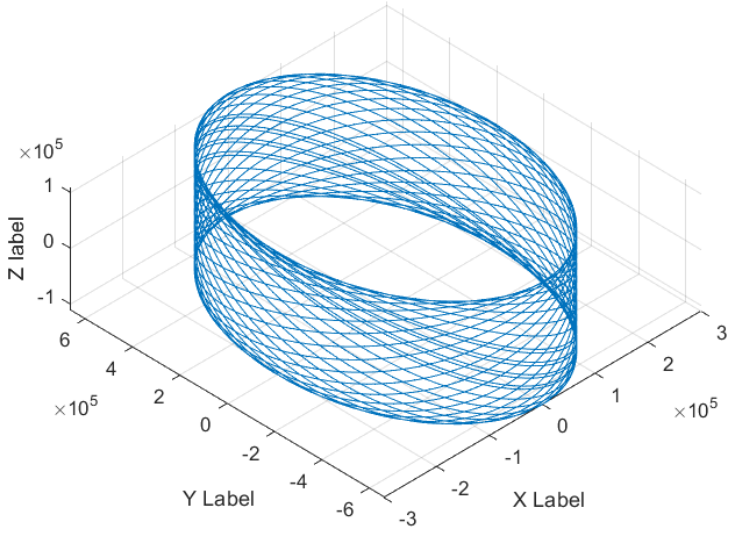

Figure 11: Lissajous type trajectories: quasi periodic halo orbits

2. When $\omega_p = \omega_v$, m=1

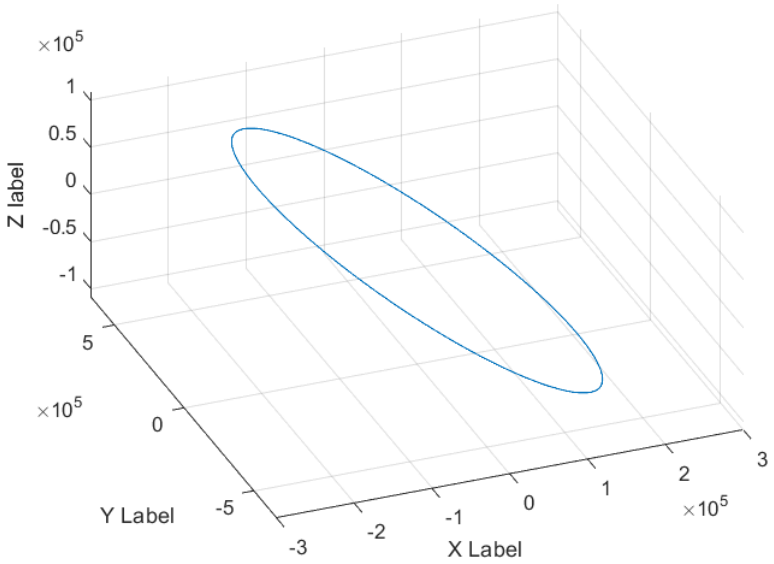

Figure 12: Northern Halo orbit, m=1

3. When $\omega_p = \omega_v$, m=3

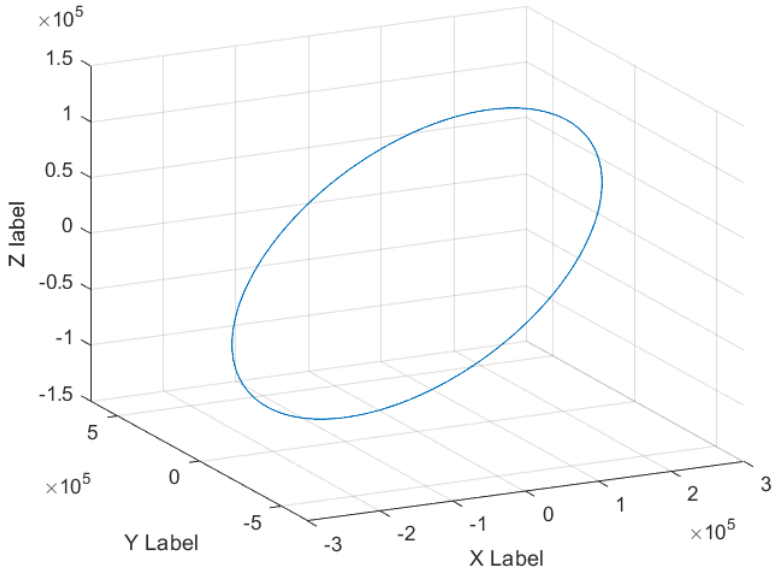

Figure 13: Southern Halo orbit, m=3

7.2 Numerical Computation

Analytical solutions cannot provide accurate solutions to motion around L1 and L2 points. Analytical approximations must be combined with numerical techniques to generate a halo orbit accurate enough for mission design.

7.2.1 Periodic Halo Orbits

Characteristics of a simple periodic halo orbit:

- The orbit always pierce the X–Z plane orthogonally, even initially at t0
- After half the period, the orbit must again cross the X–Z plane orthogonally i.e at T/2.

So, the state vectors at t0 and at half period (T/2) are:

$$X(t0) = [x_o, 0, z_o, 0, \dot{y_o}, 0]$$

$$X(T/2) = [x_{T/2}, 0, z_{T/2}, 0, \dot{y_{T/2}}, 0]$$

The end goal is to obtain values of initial conditions $[x_o, z_o, \dot{y_o}]$ such that orthogonal crossing at T/2 is ensured.

7.2.2 Differential Correction Technique

Richardson (1980) developed the third order analytical solution for the halo orbit design. But, when numerically integrated under the CR3BP model, this design is not periodic. Therefore, we make corrections to these initial conditions using Differential Correction technique. Using this closed form solution as the initial guess, the DC scheme refines the design to make it periodic.

Procedure:

1. Take the third order solution [7] as the initial guess
2. Propagate the trajectory using CR3BP Eqs.38,39,40 and ode113
3. Note the time and the x,z velocity components at T/2 i.e when the trajectory crosses the X-Z plane, which will be when Y changes sign from positive to negative. At this point x,z velocity components will not be equal to zero and have to be driven to zero after some iterations of DC.
4. The state transition matrix $\phi(6 \times 6)$ links the deviations in the state at the final time to the deviations in the initial state.
$$\delta x(t) = \phi(t, t0)\delta x(t0) \tag{79}$$
This STM is propagated numerically form t0 to T/2 by integrating simultaneously the following 42 ODEs (6 CR3BP state equations + 36 STM equations (Appendix A of [6])):
$$\dot{x} = fx \tag{80}$$
$$\dot{\phi}(t, t0) = Df(x)\phi(t, t0) \tag{81}$$
with initial conditions,
$$x(t0) = x_o \tag{82}$$
$$\phi(t0, t0) = I_6 \tag{83}$$
The Jacobian matrix Df(x)is:
$$Df(x) = \begin{pmatrix} 0 & I_3 \\ -U & 2\omega \end{pmatrix} \tag{84}$$
where,
$$\omega = \begin{pmatrix} 0 & 1 & 0 \\ -1 & 0 & 0 \\ 0 & 0 & 0 \end{pmatrix} \tag{85}$$
$$I_3 = \begin{pmatrix} 1 & 0 & 0 \\ 0 & 1 & 0 \\ 0 & 0 & 1 \end{pmatrix} \tag{86}$$
$$U = \begin{pmatrix} U_{xx} & U_{xy} & U_{xz} \\ U_{yx} & U_{yy} & U_{yz} \\ U_{zx} & U_{zy} & U_{zz} \end{pmatrix} \tag{87}$$
Here U_{xx} and others are double partial differentials of the gravitational potential equations Eqn.41

5. Once we obtain the STM at T/2 we find the deviations required in the initial state using:

$$\delta x_f = \phi(t_f, t_0)\delta x_o \tag{88}$$

We have $\delta x_f = x_{desired}$ - x_f
Three initial states $(\delta x_o, \delta z_o, \dot{y_o})$ are available to target two final states $(\delta \dot{x_f}, \delta \dot{z_f})$. Rather than invert a two by three matrix, we fix $\delta z_o = 0$ resulting in a 2×2 matrix which can easily be inverted. Alternatively, x coordinate can also be fixed.

Using the equation below we can easily find the required deviations in inital states:

$$\begin{pmatrix} \delta x_o \\ \delta \dot{y_o} \end{pmatrix} = \begin{pmatrix} \phi_{41} - \phi_{21}\frac{\ddot{x}}{\dot{y}} & \phi_{45} - \phi_{25}\frac{\ddot{x}}{\dot{y}} \\ \phi_{61} - \phi_{21}\frac{\ddot{z}}{\dot{y}} & \phi_{65} - \phi_{25}\frac{\ddot{z}}{\dot{y}} \end{pmatrix}^{-1} \begin{pmatrix} -\dot{x}_{T/2} \\ -\dot{z}_{T/2} \end{pmatrix} \tag{89}$$

6. Change the initial states and iterate the whole process till deviations become less than 10^{-16}

7.2.3 Limitations of Differential Correction

DC scheme is a very effective and quick way to obtain halo orbits but it has some limitations:

1. It fixes one out of three unknowns. Only two of the three variables are varied.
2. A very good initial guess is required which in itself requires a very good understanding for the vast theory behind halo orbits especially third order solutions
3. Since we had fixed the z coordinate, the amplitude of the halo orbit obtained is different from the one expected. Therefore, another numerical procedure called psuedo arc length continuation method is used to generate the solution for the exact value of Z amplitude

8 Numerical Computation Results

System: Sun-Earth system
L point: L1

μ	$3.040357143 * 10^{-6}$
ω	1
r	1
L_1	0.989986
n (time step)	0.00001
DC iterations	50
Accuracy	10^{-16}

Initial guess for 1,20,000 km halo orbit at **L1 point** in **Sun-Earth System** is taken according to third order solution provided by Richardson[7] and in [6]

x_o	0.9888383910739
y_o	0
z_o	0.0008152222855
$\dot{x_o}$	0
$\dot{y_o}$	0.0089606022073
$\dot{z_o}$	0

Below are the graphs obtained:

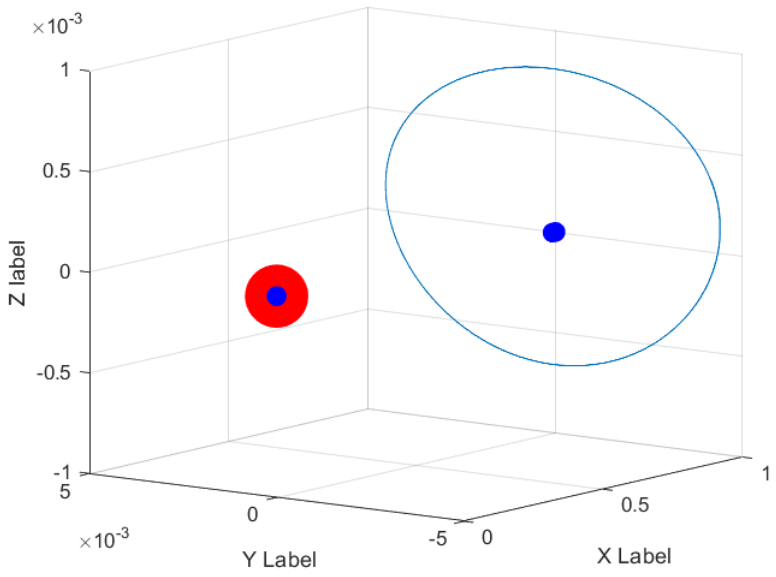

Figure 14: Halo orbit at L1 point, Sun-Earth System

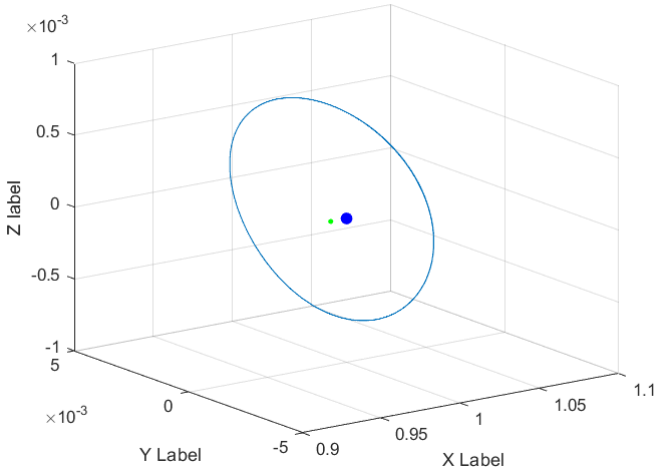

Figure 15: Close up near L1 point

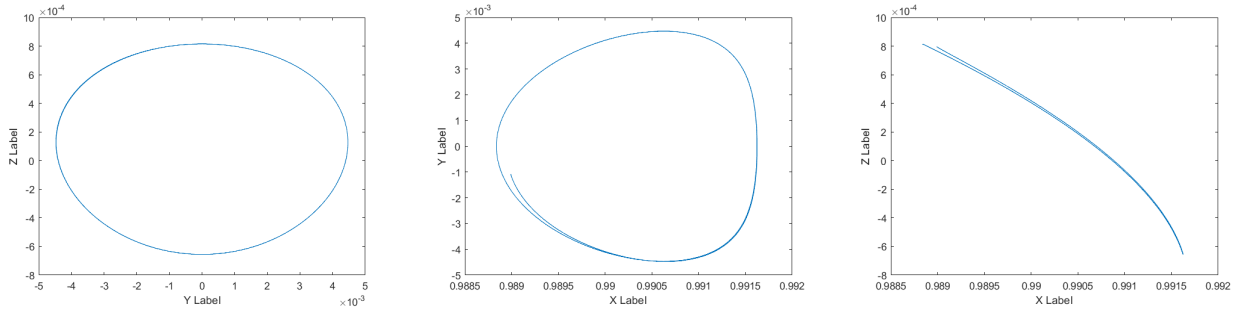

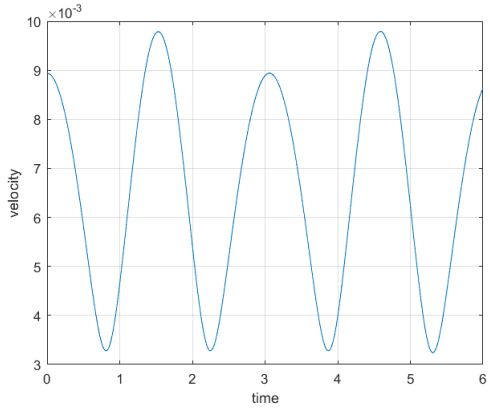

Figure 16: Velocity Profile (Barycentric)

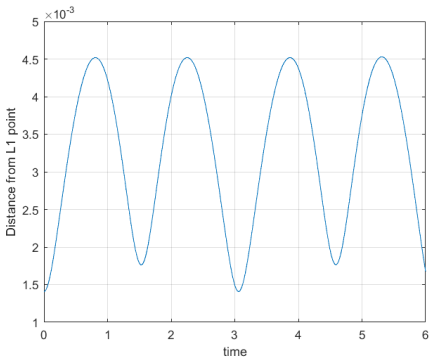

Figure 17: Distance from L1 point

The final inital conditions are:

x_o	0.988837248611012
y_o	0
z_o	0.0008152222855
$\dot{x_o}$	0
$\dot{y_o}$	0.008940287108425
$\dot{z_o}$	0

Note that all results are obtained in normalized units.

9 Discussion

- A high accuracy of 10^{-16} is required to obtain very good results. Even an accuracy of 10^{-7} is not enough for forming a periodic halo orbit in second rotation
- The smaller the step size and the more the number of Differential Correction iterations, the better are the results
- The initial guess has to be close to the solution because DC is only a correction step. That is why Richardson third order solution is taken as the initial guess. A deviation of initial conditions by fourth order can lead to increase in the DC iterations and further decrease in step size, which can make computational time very high. DC might not be able to correct an initial condition deviation of second order
- The integration is performed using ode113. Initially ode45 was used, but was replaced with ode113, as it is more accurate

Future task:

1. The code currently works for a specific amplitude of ISEE3 mission. Automating the code for any set of amplitudes and good initial guess could be the next step
2. Having designed a halo orbit, transfer trajectories from Earth to Halo orbit needs to be studied, eventually entering into stable/unstable manifolds which is the next step towards designing an interplanetary superhighway

10 Acknowledgements

I would like to express my special gratitude to my project guide Prof. Rohit Gupta for giving me the opportunity to work on such an interesting topic and guiding me throughout this project and carrying interesting discussions which made this learning experience an enriching one.

11 References

References used in making this report are:

1. Matthew M. Peet, The orbital mechanics of space elevator launch systems, Acta Astronautica 179 (2021) 153–171
2. $https://phys.org/news/2021-09-gas-station-space.html$
3. Thesis by Raoul R. Rausch, EARTH TO HALO ORBIT TRANSFER TRAJECTORIES
4. Pawan M S, Gnanaesh C M, Design and Analysis of Halo orbits around L1 Libration point for Sun Sun-Earth system
5. M. Shirobokov, Libration Point Orbits and Manifolds: Design and Station-Keeping
6. R.V. Ramanan and Pranav Nath, Precise Halo orbit Design and Optimal Transfer to Halo Orbits from Earth Using Differential Evolution. Advances in Space Research 57 (2016) 202–217
7. David L. Richardson, Halo Orbit Formulation for the ISEE-3 Mission
   J. Guidance and Control, Vol.3, No.6, Nov-Dec.1980, Article No, 80-4122
8. Wang Sang Koon, Martin W. Lo, Jerrold E. Marsden, Shane D. Ross
   Dynamical Systems, the Three-Body Problem and Space Mission Design
9. Hanspeter Schaub and John L. Junkins, Analytical Mechanics of Space Systems Second Edition, AIAA Education Series
10. Howard D Curtis, Orbital mechanics for engineering students-Elsevier, Butterworth-Heinemann (2020), (Elsevier Aerospace Engineering Series)
11. Excerpt from "A Mathematical Introduction to Robotic Manipulation" by R.M.Murray, Z. Li and S.S.Sastry
12. Andrew Torricelli, Development of CR3BP, ER3BP and N-Body Orbit Simulations Using Matlab, International Journal of Scientific Engineering Research, Volume 8, Issue 5, May-2017
13. Martin W. Lo, The InterPlanetary Superhighway and the Origins Program
14. $https://www.researchgate.net/figure/a-Orbit-of-quasi-Hilda-comet-P-Oterma-in-sun-centered-inertial-frame-during-time_fig4_28593521$
15. Martin W. Lo, The Interplanetary Superhighway and Human Habitation on the Moon
    Habitation 2006 Conference,February 5-8, 2006, Orlando, Florida

12 Appendix

12.1 MATLAB code: Halo orbit computation

12.1.1 Propagator_DC.m

```
%Normalized variables
%mu = M_earth/M;
mu = 3.040357143 * 10^-6;
omega = 1;

%correct normalization, identification of constants for a system is extremely imp

%Centered at barycentre
r = 1;
x_1 = -mu;
x_2 = 1- mu;

L_1 = 0.989986;
x0 = 0.9888383910739;
y0 = 0;
z0 = 0.0008152222855;
x0_dot = 0;
y0_dot =0.0089606022073;
z0_dot = 0;

pos_sun = [x_1, 0, 0];
pos_earth = [x_2, 0, 0];

for repeat=1:50

    %define tstart, tend and the number of time steps you want to take, n:
    tstart = 0;
    tend = 3.5;
    n = 0.00001;
    tspan = linspace(tstart,tend,tend/n);
    %define the initial conditions making sure to use the right ordering
    xinit = [x0, x0_dot,  y0, y0_dot, z0, z0_dot];

    OPTIONS = odeset('RelTol',3e-14,'AbsTol',1e-16);

    [t,x] = ode113(@ode_orbitdynamics_nonlinear, tspan, xinit, OPTIONS);
    %define the output variables:
    X = x(:,1);
    X_dot = x(:,2);
    Y = x(:,3);
    Y_dot = x(:,4);
    Z = x(:,5);
    Z_dot = x(:,6);
```

```
index = find(Y < 0, 1, 'first');
T_half = n*(index-1); %check

v_r = [X, Y, Z];
r_1 = v_r - pos_sun;
r_2 = v_r - pos_earth;
r1 = (r_1(:,1).^2 + r_1(:,2).^2 + r_1(:,3).^2).^0.5 ;
r2 = (r_2(:,1).^2 + r_2(:,2).^2 + r_2(:,3).^2).^0.5 ;

N=6;
phi_int(1:N^2)     = reshape(eye(N),N^2,1);
phi_int(1+N^2:N+N^2) = xinit;
h = 0.00001;
tspan1 = linspace(0,index*h,index);

RelTol = 3.e-14 ;
AbsTol = 1e-16;
OPTIONS = odeset('RelTol',RelTol,'AbsTol',AbsTol);

[t,phi] = ode113(@varEq,tspan1,phi_int, OPTIONS);

phi = phi(index,:);
phi  = reshape(phi(1:36),6,6);


x_half = [X(index),X_dot(index), Y(index), Y_dot(index), Z(index), Z_dot(index)];
x_desired = [0, 0]; %x_dot z_dot
del_xf = x_desired - [x_half(2), x_half(6)]; %error in final state

xdotdot = X(index) + 2*Y_dot(index) - (1-mu)*(X(index) +mu)/r1(index)^3 - mu*(X(index)
- (1-mu))/r2(index)^3 ;
zdotdot = -(1-mu)*Z(index)/r1(index)^3 - mu*Z(index)/r2(index)^3 ;

PHI11 = phi(4,1) - phi(2,1)*(xdotdot/Y_dot(index));
PHI12 = phi(4,5) - phi(2,5)*(xdotdot/Y_dot(index));
PHI21 = phi(6,1) - phi(2,1)*(zdotdot/Y_dot(index));
PHI22 = phi(6,5) - phi(2,5)*(zdotdot/Y_dot(index));
PHI = [PHI11  PHI12;
       PHI21  PHI22];


PHI_inv = inv(PHI);

del_x0 = PHI_inv*del_xf.'; %del_x0 = [del_x0, del, del_y_dot]

%changing initial state
x0 = x0 + del_x0(1);
```

```
    y0_dot = y0_dot + del_x0(2);

end

tstart = 0;
tend = 6;
n = 0.00001;
tspan = linspace(tstart,tend,tend/n);
%define the initial conditions making sure to use the right ordering
xinit = [x0, x0_dot,  y0, y0_dot, z0, z0_dot];

OPTIONS = odeset('RelTol',3e-14,'AbsTol',1e-14);
[t,x] = ode113(@ode_orbitdynamics_nonlinear, tspan, xinit,OPTIONS);
%define the output variables:
X = x(:,1);
X_dot = x(:,2);
Y = x(:,3);
Y_dot = x(:,4);
Z = x(:,5);
Z_dot = x(:,6);

Vel = (X_dot.^2 + Y_dot.^2 + Z_dot.^2).^0.5;

figure();
plot(t,Vel);
xlabel('time');
ylabel('velocity');
grid on;

figure();
plot3(X,Y,Z);
xlabel('X Label');
ylabel('Y Label');
zlabel('Z label');
grid on;

xlim([0.9 1.1]);
hold on
%scatter(pos_sun,0,1000, 'filled','r');
scatter(pos_earth,0,50, 'filled','b');
scatter(L_1,0,10, 'filled','g');
hold off
```

12.1.2 ode_orbitdynamics_nonlinear.m

```
function dxdt = ode_orbitdynamics_nonlinear(t,x)

%Normalized variables
```

```
%mu = M_earth/M;
mu = 3.040357143 * 10^-6;
omega = 1;

%Centered at barycentre
r = 1;
x_1 = -mu;
x_2 = 1- mu;

pos_sun = [x_1, 0, 0];
pos_earth = [x_2, 0, 0];

v_r = [x(1), x(3), x(5)];

r1 = norm(v_r - pos_sun);
r2 = norm(v_r - pos_earth);

%2. Define new variables: y=x(1), ydot=x(2), etc
x1 = x(1); %x
x2 = x(2); %xdot
y1 = x(3); %y
y2 = x(4); %ydot
z1 = x(5); %z
z2 = x(6); %zdot

%3. Write out your first order system of ODE's:
dxdt = zeros(size(x));
dxdt(1) = x2;
dxdt(2) = 2*y2 + (1 - (1-mu)/r1^3 - mu/r2^3)* x1 + mu*(1-mu)/r2^3 - mu*(1-mu)/r1^3;
dxdt(3) = y2;
dxdt(4) = -2*x2 + (1 - (1-mu)/r1^3 - mu/r2^3)* y1;
dxdt(5) = z2;
dxdt(6) = (- (1-mu)/r1^3 - mu/r2^3)* z1;

end
```

12.1.3 varEq.m

```
function PHIdot = varEq(t,phi)

mu = 3.040357143 * 10^-6 ;

x(1:6) = phi(37:42);
phi  = reshape(phi(1:36),6,6);

X=x(1);
Xdot = x(2);
Y=x(3);
```

```
Ydot = x(4);
Z=x(5);
Zdot = x(6);

pos_sun = [-mu, 0, 0];
pos_earth = [1-mu, 0, 0];

v_r = [X, Y, Z];
r1 = norm(v_r - pos_sun);
r2 = norm(v_r - pos_earth);

% The following are three double partial derivatives of the effective potential U(x,y)

Uxx = 1 - (1-mu)*(1 - 3*((X + mu)^2)/(r1^2))/(r1^3) - mu*(1 - 3*((X - (1-mu))^2/(r2^2))/(r2^3)) ;
Uyy = 1 - (1-mu)*(1 - 3*(Y^2)/(r1^2))/(r1^3) - mu*(1 - 3*(Y^2)/(r2^2))/(r2^3) ;
Uzz = -(1-mu)*(1 - 3*Z^2/r1^2)/r1^3 - mu*(1 - 3*Z^2/r2^2)/r2^3 ;
Uxy = 3*Y*(1 - mu)*(X + mu)/r1^5 + 3*mu*Y*(X - (1-mu))/r2^5 ;
Uyx = Uxy;
Uxz = 3*Z*(1 - mu)*(X + mu)/r1^5 + 3*mu*Z*(X - (1-mu))/r2^5 ;
Uzx = Uxz;
Uyz = 3*Z*(1 - mu)*Y/r1^5 + 3*mu*Z*Y/r2^5 ;
Uzy = Uyz;


% The following is the Jacobian matrix

        A =   [0     0      0    1  0  0;
               0     0      0    0  1  0;
               0     0      0    0  0  1;
               Uxx   Uxy   Uxz   0  2  0;
               Uyx   Uyy   Uyz  -2  0  0;
               Uzx   Uzy   Uzz   0  0  0];


phidot = A * phi; % variational equation

PHIdot        = zeros(42,1);
PHIdot(1:36)  = reshape(phidot,36,1);
PHIdot(37)    = x(2);
PHIdot(38)    = 2*Ydot + (1 - (1-mu)/r1^3 - mu/r2^3)* X + mu*(1-mu)/r2^3 - mu*(1-mu)/r1^3;
PHIdot(39)    = x(4);
PHIdot(40)    = -2*Xdot + (1 - (1-mu)/r1^3 - mu/r2^3)* Y;
PHIdot(41)    = x(6);
PHIdot(42)    = (- (1-mu)/r1^3 - mu/r2^3)* Z;

end
```